Vacuum 224 (2024) 113189

Contents lists available at ScienceDirect

Vacuum

journal homepage: www.elsevier.com/locate/vacuum

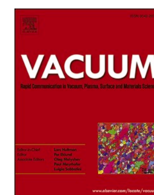

Effect of 710 MeV Bi^{+51} swift heavy ions irradiation on Se pre-implanted polycrystalline SiC

T.S. Mabelane [a,*], M. Sall [b], Z.A.Y. Abdalla [a], V.A. Skuratov [c,d,e], T.T. Hlatshwayo [a]

[a] Physics Department, University of Pretoria, Pretoria, South Africa
[b] CIMAP Normandie Univ, CEA, CNRS, ENSICAEN, UNICAEN, 14000, Caen, France
[c] Joint Institute for Nuclear Research, Dubna, Russia
[d] Dubna State University, Dubna, Moscow Region, Russia
[e] National Research Nuclear University MEPhI, Moscow, Russia

ARTICLE INFO

Handling Editor: Prof. L.G. Hultman

Keywords:
Implantation
Irradiation
SiC
Se
Amorphization
Recrystallization

ABSTRACT

In this study, the effect of swift heavy ions (SHIs) irradiation in the recrystallization of polycrystalline SiC pre-implanted with selenium (Se) ions and migration of Se was investigated. The main objective of this study is to investigate the role of SHIs with the maximum electronic energy loss greater than 20 keV/nm on structural evolution of initially amorphized pre-implanted SiC and the migration of pre-implanted fission products (FPs). The pristine SiC samples were first implanted with 200 keV Se ions to a fluence of 1×10^{16} cm^{-2} at room temperature (RT) and at 350 °C. Some of the pre-implanted samples were then irradiated with bismuth (Bi) ions of 710 MeV to a fluence of 1×10^{13} cm^{-2} at RT. The characterization of both the implanted and implanted then irradiated SiC was conducted using techniques such as transmission electron microscopy (TEM), Raman spectroscopy, scanning electron microscopy (SEM), and Rutherford backscattering spectrometry (RBS). At RT, Se ions implantation caused the amorphization of SiC to a depth of about 187 nm beneath the surface. In contrast, when implanted at 350 °C, the SiC retained its crystalline structure with some defects (i.e., point defects, point defect clusters and some dislocation loops). The SHIs irradiation of the RT implanted SiC resulted in the reduction of the amorphous layer thickness from 187 nm to around 178 nm and led to the formation of nanocrystalline SiC in the amorphous layer. Irradiation of the SiC implanted at 350 °C induced some crystallization of defects. Notably, no evidence of Se ions migration was observed in both the irradiated RT-implanted and the hot-implanted SiC.

1. Introduction

About two thirds (~63.3%) of the global electricity is produced from burning of fossil fuels such as coal, natural gas, petroleum etc, with coal being a primary source [1]. Burning of fossil fuels results in emission of carbon dioxide (CO_2), thus increasing the CO_2 levels which is a major contributor to human health and welfare issues [2,3]. Therefore, development of carbon free, environmentally friendly, and sustainable forms of energy is a global imperative with hydro, wind, solar and nuclear energy as some of the proposed candidates [4]. To all these energy sources, nuclear energy is the less favoured due to safety concerns arising from the possible release of radioactive FPs to the environment and nuclear waste storage. In Modern High Temperature Gas Cooled Reactors (i.e., pebble bed modular reactor (PBMR)), the strategy for containing the FPs involves coating the fuel kernel with chemical vapour deposited (CVD) layers of carbon (C) and silicon carbide (SiC) to form a tri-structural isotropic (TRISO) particle [5,6]. The TRISO fuel particle consists of a inner UO_2 core, which is encapsulated by four distinct layers: a porous carbon buffer layer to accommodate internal gas accumulation, an inner pyrolytic carbon (IPyC) layer serving as a diffusion barrier for most non-metallic FPs, a SiC layer that functions as the primary diffusion barrier for metallic FPs, and an outer pyrolytic carbon (OPyC) layer designed to shield the SiC layer from external chemical and mechanical interactions while assisting in reducing stress within the SiC material [7]. The use of SiC is grounded in its exceptional properties, which encompass extreme hardness, high thermal conductivity, high temperature stability, radiation resistance, small neutron absorption cross-section and high corrosion resistance [8,9]. The 3C–SiC polycrystalline material stands out as the preferred polytype for applications in nuclear reactors, particularly in TRISO fuel particles. This

* Corresponding author.
E-mail address: u22019937@tuks.co.za (T.S. Mabelane).

https://doi.org/10.1016/j.vacuum.2024.113189
Received 1 November 2023; Received in revised form 11 February 2024; Accepted 29 March 2024
Available online 30 March 2024
0042-207X/© 2024 The Authors. Published by Elsevier Ltd. This is an open access article under the CC BY-NC-ND license (http://creativecommons.org/licenses/by-nc-nd/4.0/).

preference is primarily attributed to the higher radiation resistance of the 3C–SiC polytype against neutron bombardment compared to single crystals. Notably, the fabrication of 3C–SiC takes place under identical conditions as those used for producing SiC coatings on TRISO particles [10,11].

In the core of a nuclear fuel, a fission reaction takes place when a nucleus of the uranium isotope U-235 absorbs a thermal neutron, causing it to become unstable and then eventually split into two lighter nuclei/fission products (FPs). During this process, two or three neutrons are emitted, along with a huge amount of energy. The FPs dissipate different range of energies, essentially in the order of 100 MeV, followed by low keV when they have slowed down. The energies in the order of 100 MeV are comparable to the energy of swift heavy ions (SHIs)) [12]. SHIs lose most of their energy via electronic energy loss as they are traversing the target material until they have slowed down to the low energies i.e., keV region, where they lose their energy via nuclear energy loss [13]. Therefore, during operation of fission nuclear reactor, SiC will also be irradiated with SHIs. The irradiation of SiC with SHIs might have some role in the containment of FPs in TRISO particle where SiC is the main diffusion barrier. Hence, it is essential to understand the role of SHIs in the migration behaviour of FPs.

The effect of SHIs irradiation on SiC pre-implanted with low energy ions has been reported by Audren et al. [14]. In this study, 700 keV iodine was implanted into SiC at RT and elevated temperatures (400 °C and 600 °C) to fluence of 10^{15} cm^{-2}. The elevated temperature (i.e., 600 °C) implanted sample was subsequently irradiated with either Au ions of 6.8 MeV or 104 MeV Pb ions (of maximum electronic energy loss of ~4.1 or 18.9 keV/nm) at 600 °C. The results revealed no migration of implanted iodine induced by SHIs irradiation.

The recrystallization of pre-damaged SiC caused by SHIs irradiation was reported by Benyagoub et al. [15,16]. In this previous study, the 700 keV iodine was pre-implanted into SiC substrate to fluences of 7.5×10^{13} and 1.1×10^{14} cm^{-2}, subsequently irradiated with 827 MeV Pb ions (of maximum electronic energy loss ~ 33 keV/nm) at RT. Implanting SiC to a fluence of 7.5×10^{13} cm^{-2} introduced some defects, mainly point defects, into the SiC structure, while implanting it to a fluence of 1.1×10^{14} cm^{-2} led to the amorphization of SiC. Subsequently, irradiating the pre-implanted SiC with SHIs resulted in the epitaxial growth of the amorphous layer, and almost total recovery of the defects was observed in the initial SiC structure with defects. Slight annealing effect has also been observed after exposing pre-damaged SiC to 50 MeV I ions to fluence of 10^{13} cm^{-2} [17]. However, the damage recovery was not significant compared to the one observed in Refs. [15,16], probably due to electronic energy loss difference-with 50 MeV I ions having only 12 keV/nm which is well less than the one generated by 827 MeV Pb ions (~33 keV/nm).

Quite recently our group started investigating the effect of SHIs irradiation on SiC pre-implanted with fission products surrogates (i.e., Kr, Sr, I, Xe and Ag) of nuclear safety concern [7,12,13,18]. In these previous investigations, the pre-implanted SiC samples were irradiated with Xe ions of 167 MeV equivalent to maximum electronic energy loss of about 20 keV/nm. Regardless of the chemistry of the pre-implanted FPs surrogates the results revealed that SHIs irradiation of the RT implanted resulted in some limited epitaxial growth of the amorphized layer accompanied by the formation of nano-crystallites embedded in the amorphous SiC structure owing to electronic energy deposition by SHIs. The SHIs interact with the electrons of the irradiated substrate, resulting in the kinetic energy being transferred into electrons of the substrate which then transfer the kinetic energy into the substrate atoms via electron-phonon interaction. This process results in a rapid and notable rise in the lattice temperature. When the lattice temperature surpasses the melting point of the material, a transition from solid to liquid phase along the trajectory of the ions can take place. This mechanism is explained within the framework of the inelastic thermal spike model [19]. No migration of the pre-implanted FPs was detected after SHIs irradiation.

To the best of our knowledge, the role of SHIs with the maximum electronic energy loss greater than 20 keV/nm in structural evolution of initially amorphized-pre-implanted SiC and the migration of pre-implanted FP has only been investigated for iodine pre-implanted SiC [15,16]. For the safety of the nuclear reactors, similar investigation needs to be undertaken for all other important FPs. Hence, in this study, the role of SHIs (with maximum electronic energy loss greater than 20 keV/nm) irradiation in the structural evolution and migration in the SiC pre-implanted with Se ions was investigated.

Selenium (Se) is a non-metallic element with nine major radioactive isotopes of which only one- Se-79 has a concerning long half-life of 3.8×10^5 years, which was recently updated [20,21]. Se-79 is a constituent found in spent nuclear fuel and radioactive waste materials linked to the operation of nuclear reactors. It is generated with an approximate yield of 0.04% per fission event. It emits a beta particle during its radioactive decay which pose a major health concern (i.e., likelihood of inducing cancer) when absorbed by a human body [3]. Thus, containment of Se in the nuclear reactor is crucial. Recent studies on the microstructural properties of Se implanted into polycrystalline SiC have been reported by Refs. [22–24]. Their findings showed that Se implantation at RT amorphized SiC near the surface region, while hot implantation (350 and 600 °C) retained crystalline structure of SiC with some structural defects (i.e., predominately, point defects).

In this work, Se ions of 200 keV were first implanted into SiC wafers at both RT and 350 °C, to a fluence of 1×10^{16} cm^{-2}. Subsequently, some of the pre-implanted SiC samples were exposed to Bi ions of 710 MeV, to a fluence of 1×10^{13} cm^{-2} at RT. The only implanted samples and implanted then irradiated samples were characterized using TEM, Raman spectroscopy, SEM, and RBS. Since the Bi ions used in this study have the maximum electronic energy loss of about ~33.7 keV/nm that is greater than that of 167 MeV Xe ions of about 20 keV/nm used in the earlier studies, the findings of this study were compared with Xe irradiated samples in Refs. [7,12–18] to investigate the impact of electronic energy loss in the recrystallization of the damaged SiC.

2. Experimental procedure

In this study, polycrystalline SiC wafers primarily comprised of 3C–SiC, with minor traces of 6H–SiC [22], were sourced from Valley Design Corporation. The microstructure of the original wafers was examined using scanning electron microscopy (SEM) and electron backscatter diffraction (EBSD). The analysis revealed that the SiC wafers mainly consist of columnar crystallites oriented along the growth direction with diameters of a few micrometres. Additionally, smaller crystals which do not align parallel to the columns were observed. EBSD analysis indicated a predominant cubic lattice structure, although some hexagonal growth modes were also identified [25]. An implanter at Friedrich-Schiller University, Germany was used to implant Se ions. The implantation was conducted at RT and at 350 °C, both under vacuum conditions, with an energy of 200 keV and a fluence of 1×10^{16} cm^{-2}. Subsequently, certain pre-implanted SiC wafers underwent irradiation with 710 MeV Bi^{+51} at RT, to a fluence of 1×10^{13} cm^{-2}, using the IC-100 FLNR cyclotron at the Joint Institute for Nuclear Research (JINR) in Dubna, Russia.

Both RT and 350 °C only implanted and pre-implanted then 710 MeV Bi^{+51} irradiated SiC were characterized through multiple techniques, including Raman spectroscopy, transmission electron microscopy (TEM), Rutherford backscattering spectroscopy (RBS) and scanning electron microscopy (SEM). The Witec alpha 300 RAS + Raman spectrometer was used in this study. The Raman spectra were obtained using an excitation laser with wavelength of 532 nm (visible range of electromagnetic spectrum), and power laser of 2.5 mW. The changes in the morphology of the SiC surfaces were assessed by employing a Zeiss Ultra 55 field emission gun scanning electron microscope (FEG-SEM) equipped with an in-lens detector. An acceleration voltage of 2 kV was applied during the analysis. To track the migration of the implanted Se ions both

before and after irradiation, RBS was employed. Analysis was conducted using 2 MeV helium ions (He^+), and the backscattered ions were detected by a silicon (Si) surface barrier detector at a scattering angle of 150°. Throughout the measurements, a constant current of approximately 500 pA was maintained, and a total charge of 500 nC was collected per measurement. The backscattered energy in channel number of the Se profile was converted into depth utilizing Ziegler, Biersack, and Littmark (ZBL) stopping powers [26], along with the density of pristine SiC (3.21 g/cm^3). The RBS spectra showed that the conversion of channels into depth scale had no effect on the original Se profiles (see Fig. S1 in the supplementary data). The microstructural evolutions in the only implanted and pre-implanted then irradiated samples were characterised using TEM. TEM lamellas were prepared for cross-sectional observations with the focused-ion-beam (FIB) method using 30 keV Ga^+ ions in a Helios Nanolab 660 system (Thermofisher). The ion energy was decreased to 2 keV in several steps to obtain samples with thicknesses lower than 100 nm. Finally, the samples were cleaned with a plasma cleaner immediately before being measured. A JEOL-F200 TEM with a cold field emission electron gun operating at 200 kV was used to analyse the prepared specimens.

3. Results and discussions

Before performing implantation and irradiation experiments, the simulations of ions in SiC were performed using the stopping and range of ions in matter (SRIM) 2012 in a full damage cascade mode [26]. In these simulations, displacement energies of 20 eV for carbon (C) and 35 eV for silicon (Si) were employed, along with a SiC material density of 3.2 g/cm^3 [27]. Fig. 1 shows the relative atomic density (RAD) (%), displacement per atom (dpa), and electronic energy loss versus depth obtained from SRIM simulations for implanted Se ions and irradiated Bi ions. The RAD (%) was calculated as the ratio of density of implanted ions to density of the substrate as shown in equation (1):

$$RAD\ (\%) = \frac{\rho_{ions}}{\rho_{SiC}} \times 100 \tag{1}$$

While the fluence was converted into *dpa* using equation (2):

$$dpa = \frac{\frac{vac}{ion\ (\text{Å})} \times 10^8}{\rho_{SiC}(atoms/cm^3)} \times \varphi(ions\,/\,cm^2) \tag{2}$$

where φ is the ion fluence, ρ_{SiC} is the theoretical atomic density of silicon carbide (9.641 × 10^{22} atoms/cm^3) and *vac/ion* is the vacancy per ion ratio from SRIM.

Fig. 1 shows the SRIM simulated results together with Se depth profiles from RBS. Se ions of 200 keV has maximum nuclear energy loss of about 1.73 keV/nm which is far greater than the maximum electronic energy loss of about 0.5334 keV/nm. Conversely, Bi ions of 710 MeV has maximum electronic stopping power of ~33.7 keV/nm which is far greater than their maximum nuclear stopping power ~0.0808 keV/nm. The critical dpa to amorphize SiC being 0.3 dpa [28], implantation of 200 keV Se ions will result in an amorphous layer of about 150 nm as shown in Fig. 1 (b) while 710 MeV Bi ions will not amorphize SiC as shown in Fig. 1 (c), as even the maximum damage of 710 MeV Bi ions (of about 0.0018 dpa) is less than the amorphization threshold of SiC. However, in this study, Bi ions were used to irradiate the Se-pre-implanted SiC. This will result in the amorphous SiC layer retained by Se ions implantation being exposed to electronic energy loss. Hence, some microstructural evolution in the irradiated, initially amorphized SiC irradiated with SHIs of maximum electronic energy loss less than 33.7 keV used in the current study [7,12,13,18]. Moreover, all

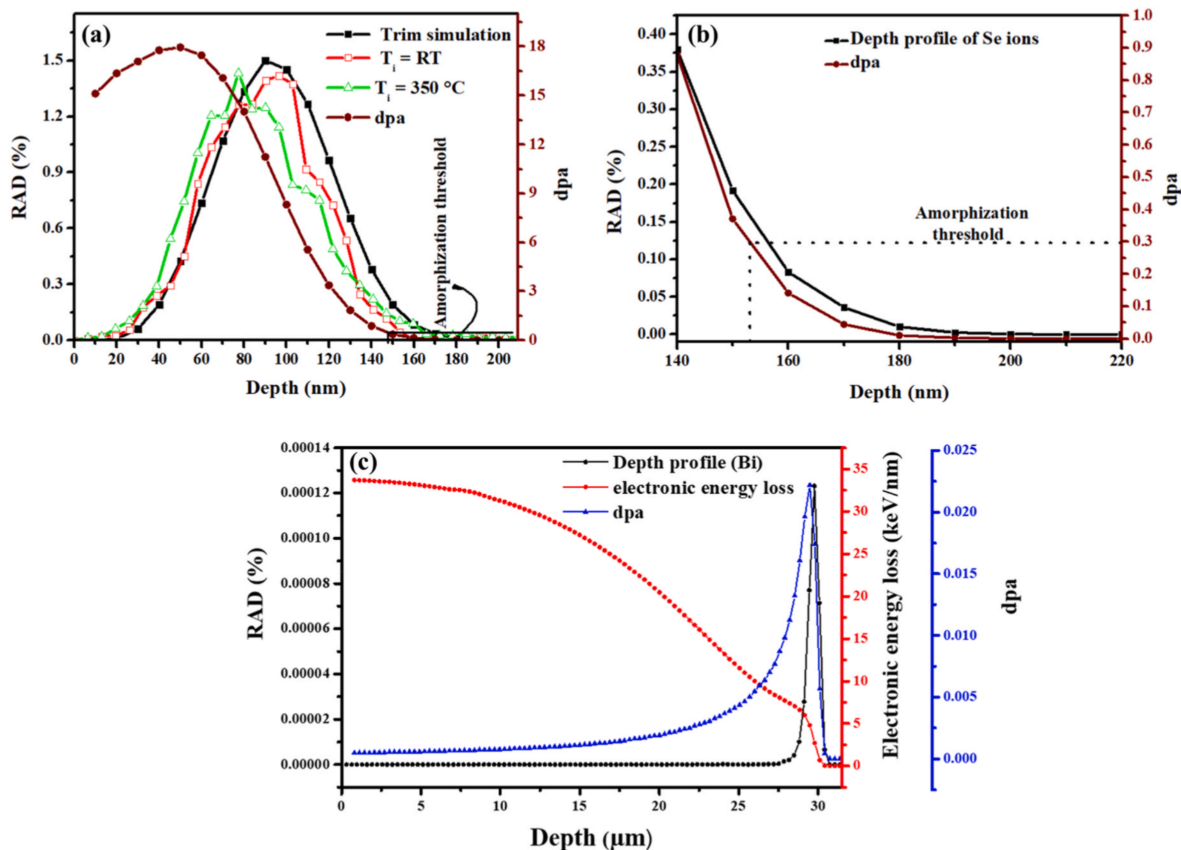

Fig. 1. The relative atomic density (%) and displacement per atom (dpa) versus depth obtained from RBS experiments and SRIM simulations for (a) implanted Se ions to fluence of 1 × 10^{16} cm^{-2} at RT and 350 °C, (b) zoomed in version of (a) and (c) Bi ions irradiation to fluence of 1 × 10^{13} cm^{-2} and the electronic energy loss for 710 MeV Bi ions.

Se depth profiles (see Fig. 1 (a)) obtained from RBS of the Se ions implanted into SiC at different temperatures are almost Gaussian with projected range of 89.2 nm which is in reasonable agreement with the projected range of the simulated Se ions of ~89.6 nm.

TEM micrographs of the RT implanted SiC before (a) and after (b) SHIs irradiation are shown in Fig. 2 together with the selected area diffraction (SAD) patterns of their damaged and bulk (unirradiated) regions. The double red arrow indicates the damaged SiC layer. The layer on the surface is a protective platinum (Pt) layer deposited by electron beam and gallium Ga ions. The significance of this protective layer lies in its capability to shield the surface of the specimen within the selected lamella area from potential damage caused by ion beams. Additionally, it serves to prevent inadvertent grinding during the lamella preparation process. Implantation of Se ions retained a damage layer of about 187 nm below surface. Its corresponding SAD pattern shows a diffuse halo ring indicating amorphous SiC structure. SHIs irradiation of RT implanted SiC caused epitaxial growth of the amorphous SiC from amorphous-crystalline interface resulting in the reduction in the amorphous SiC layer from 187 nm to 178 nm. Furthermore, randomly oriented nano-crystallites, observed with Fresnel contrast, are present in this region (highlighted in blue circles) [13,18]. Therefore, SHIs irradiation caused epitaxial growth accompanied by a partial recrystallization within the previously amorphized layer. Similar recrystallization behaviour has been reported [7,13,18] for SiC pre-implanted with low energy ions at RT followed by 167 MeV Xe^{+26} irradiation at RT (maximum electronic energy loss of 20 keV/nm) to fluences of 3.4×10^{14} cm^{-2} and 8.4×10^{14} cm^{-2}. However, in this study the recrystallization is taking place at lower fluence of 1×10^{13} cm^{-2} which might be due to high maximum electronic energy loss of 33.7 keV/nm as compared to 20 keV/nm used in the previous studies. Hence it can be deduced that the dose of electronic stopping energy loss (over 20 keV/nm) has a significant impact on the recrystallization behaviour of defective SiC.

Fig. 3 shows the TEM micrographs and SADs of the 350 °C-implanted SiC before (a) and after (b) SHIs irradiation. Implantation at 350 °C resulted in the implanted region composed of the less defective and highly defective layer. The highly defective layer primarily exhibits point defects with some point defect clusters and dislocation loops, while the less defective layer is characterized by stacking faults and dislocations [29]. The defective layers are indicated by the blue (less defective layer) and red (highly defective layer) double arrows in Fig. 3. The less defective layer is about 70 nm from the surface and the highly defective layer is ~95 nm (from 70 nm below the surface) constituting to a total defective SiC layer of about 165 nm. The lack of amorphization in SiC implanted at 350 °C was expected since the temperature of irradiation is above the critical amorphization temperature of SiC (of about 300 °C) [29]. Comparing the TEM results with results in Fig. 1 (a), it becomes evident that most of the implanted Se ions are in the high defective region which might also be a highly strained region owing to the implanted ions [30]. SHIs irradiation of the 350 °C implanted SiC caused the migration of defects in the implanted layer resulting in the reduction of the less defective region to about 47 nm from the surface and highly defective region to 75 nm from the less defective region. Moreover, the highly defective region seems to have moved towards the surface. The reduction in the highly defective region is due to recrystallization. While the reduction in the less defective region and the movement of the highly defective region is due to the migration of defects. The defects migration rate is more on the pristine and highly defective region, hence the reduction from the back. However, if one compares the remaining defective region with results in Fig. 1, the remaining defective region is still the region with majority of Se atoms. Therefore, the effect of strain filed might not be ruled out. Similar recrystallization behaviour of defects in SiC was reported for iodine ions of 700 keV implanted into SiC subsequently irradiated with 827 MeV Pb ions (maximum electronic energy loss of about ~33 keV/nm) to fluence of 2×10^{13} cm^{-2} [15,16]. In the current study the SiC with defects was irradiated with 710 MeV Bi ions (maximum electronic energy loss of 33.7 keV/nm) to fluence of 1 × 1013 cm-2 which is quite comparable to Refs. [15,16], hence consistency in these two results was expected.

Fig. 4 shows the Raman spectra of pristine SiC, and RT and 350 °C

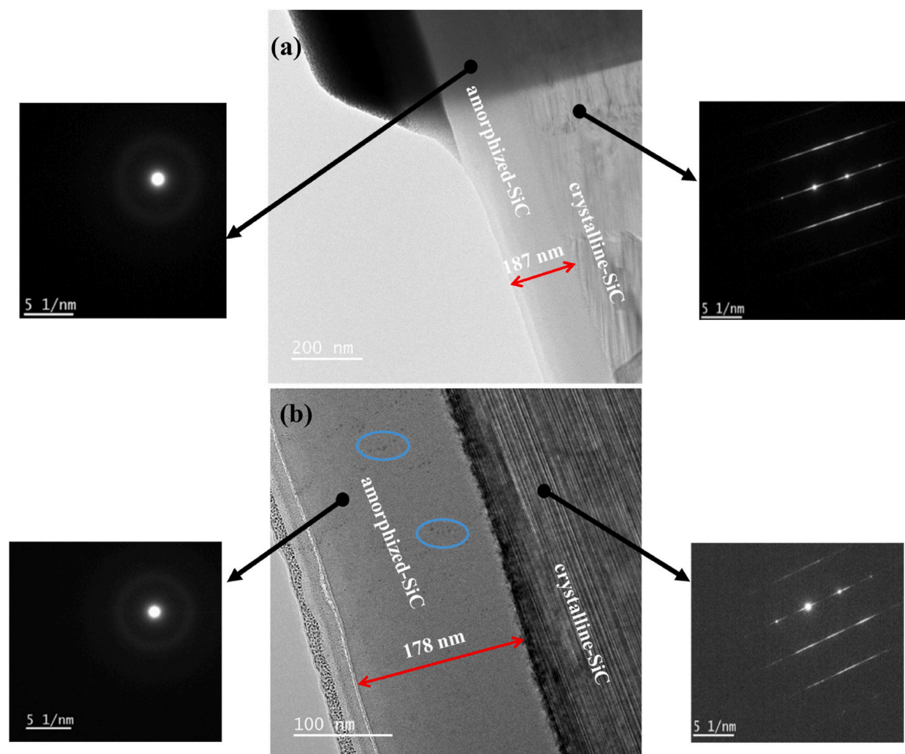

Fig. 2. TEM micrographs of (a) as-implanted polycrystalline SiC at room temperature and subsequently (b) irradiated with SHIs. The SADs of amorphous and bulk (crystalline) are also incorporated. Areas where the SADs were taken are indicated with arrows.

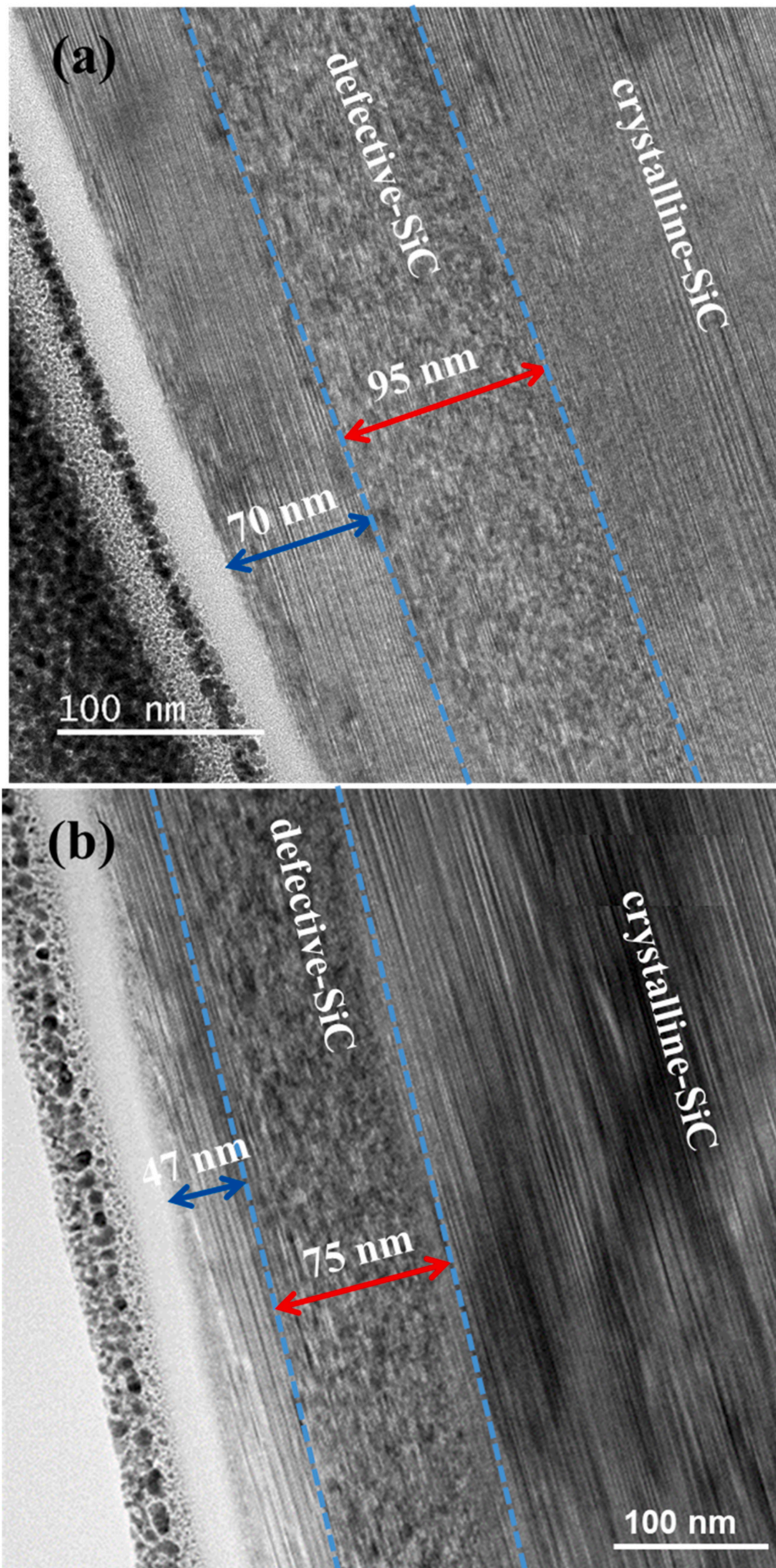

Fig. 3. TEM micrographs of (a) as-implanted polycrystalline SiC at 350 °C and subsequently (b) irradiated with SHIs.

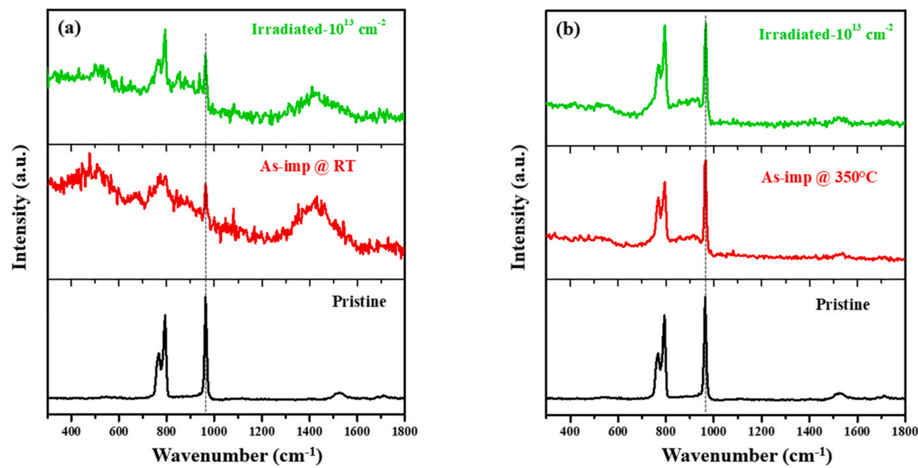

Fig. 4. Raman spectra of the Se implanted samples at (a) RT, and (b) 350 °C and after irradiation. Pristine spectrum was included for comparison.

implanted SiC before and after irradiation. The Raman spectrum of pristine SiC has vibration modes at (~765 and 791 cm^{-1}) and 965 cm^{-1} belonging to transverse optical mode (TO) and longitudinal optical mode (LO), respectively [31], indicating that the pristine SiC is composed of 3C–SiC with some traces of 6H–SiC [32]. Implantation of Se ions at RT resulted in broadening of Raman characteristic peaks of SiC and appearance of Si–Si (~525 cm^{-1}) and *C*–C (~1425 cm^{-1}) peaks, indicating amorphization of SiC which coincide with previous findings [22–24]. The irradiation of SiC implanted at RT with SHIs led to a partial reappearance of SiC characteristic Raman peaks (between 700 and 1100 cm^{-1}). However, the Si–Si (~525 cm^{-1}) and C–C (~1425 cm^{-1}) peaks were still present after irradiation, indicating limited recrystallization of the initially amorphized SiC layer. This limited recrystallization was attributed to the thermal spikes induced by the electronic energy loss [19,33]. These observations correlate with previous reported work [7,12,18,33] in which an amorphized SiC due to low energy ion implantation at RT were subjected to 167 MeV Xe^{+26} irradiation at RT (maximum electronic energy loss of 20 keV/nm) to fluences of 3.4 × 10^{14} cm^{-2} and 8.4 × 10^{14} cm^{-2}. In the current study, the amorphous SiC was exposed to lower fluence of 1 × 10^{13} cm^{-2} of Bi ions, nonetheless, recrystallization was observed which might be attributed to high maximum electronic energy loss of 33.7 keV/nm as compared to 20 keV/nm used in the previous studies.

Implantation at elevated temperature caused only the reduction in Raman characteristic peaks of SiC indicating accumulation of defects without amorphization [22]. This is in line with TEM results discussed earlier in Fig. 3. The irradiation of pre-implanted SiC with SHIs led to a narrower full width at half maximum of LO mode compared to Se ions only implanted SiC, indicating partial recrystallization of the initially retained defects. The vertical dashed line indicates the centre of LO mode peak, which was used to monitor the Raman shift. There was no Raman shift observed after SHIs irradiation, suggesting lack of tensile or compressive stress within the subsurface of the materials. The observed results are in good agreement with the reported TEM (in Figs. 2 and 3).

The SEM micrographs of implanted and implanted then irradiated SiC are shown in Fig. 5. SEM surfaces of pristine SiC, RT and 350 °C Se ions only implanted SiC were recently reported by Ref. [22]. Their results showed that the pristine surface had polishing marks which were mechanically induced during the polishing process. Implantation of 200 keV Se ions at RT led to flat and featureless surface, indicating, sputtering of the surface atoms as a result of bombarding them with energetic ions, and the swelling of the amorphous SiC. Implantation at elevated temperature resulted in the reduced polishing marks and appearance of some grains, indicating the presence of crystalline structure. SHIs irradiation of RT pre-implanted SiC resulted in the appearance of polishing marks (see Fig. 5 (a)) on the initially flat and featureless surface. However, these polishing marks are less noticeable compared to those observed in the pristine SiC surface. Meanwhile, subjecting the 350 °C pre-implanted SiC to SHIs irradiation caused the appearance of more pronounced polishing marks and grains. Both SEM results of the SHIs irradiated samples indicate recrystallization of some defects in line with TEM and Raman results discussed earlier.

The effect of SHIs irradiation on the migration behaviour of Se ions implanted into SiC was studied using RBS. The Se depth profiles obtained from RBS both before and after SHIs irradiation are displayed in Fig. 6. RBS did not reveal any substantial or measurable broadening and shifting in the Se profile, indicating that there was no detectable migration of the implanted Se ions after SHIs irradiation. This lack of detectable migration after irradiation was also observed by Refs. [12,13,18] for silver, krypton, and xenon ions of 360 keV pre-implanted into polycrystalline SiC, subsequently irradiated with 167 MeV Xe ions of maximum electronic energy loss of 20 keV/nm. The similarity in the current finding and those from previous studies suggests that the maximum electronic energy loss over 20 keV/nm does not influence the

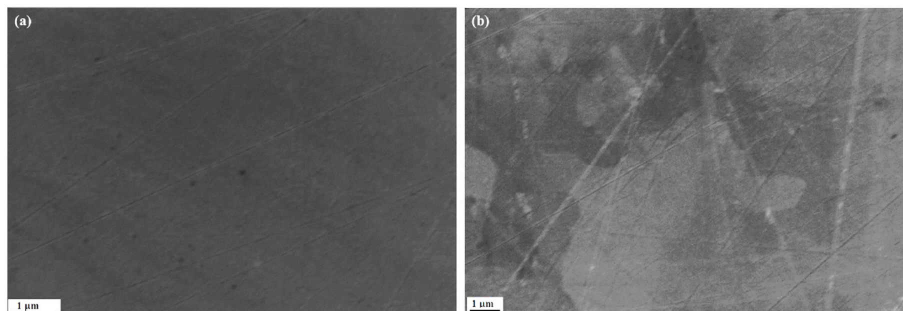

Fig. 5. SEM micrographs of the Se-implanted then SHIs irradiated SiC at (a) RT and (b) 350 °C.

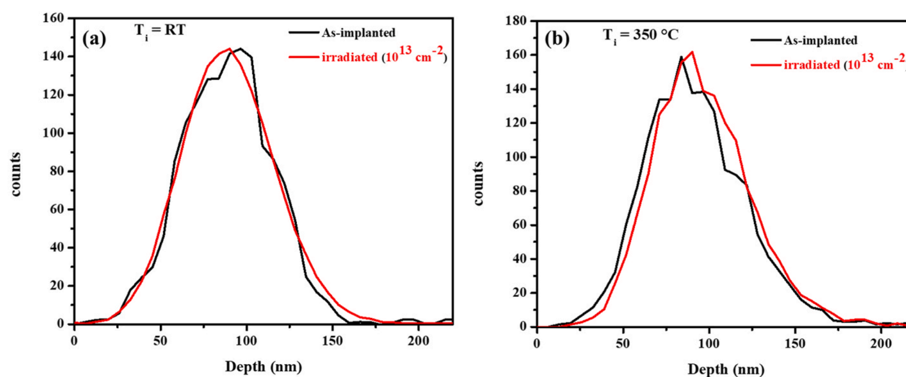

Fig. 6. Se depth profiles from RBS of SiC implanted at (a) RT, and (b) 350 °C before and after SHIs irradiation.

migration of implanted FPs.

4. Summary

This study delved into the effect of subjecting Se-implanted SiC to SHIs (710 MeV Bi^{+51}) irradiation, exploring both the microstructural changes of Se implanted SiC and migration behaviour of Se ions within the SiC material. The 200 keV Se ions were implanted into polycrystalline SiC to fluence of 1×10^{16} cm^{-2} at RT and 350 °C, following this, certain pre-implanted SiC underwent irradiation with 710 MeV Bi^{+51} to fluence of 1×10^{13} cm^{-2} at RT. The microstructural evolutions were monitored with TEM, Raman, and SEM, while the migration of the implanted Se ions was tracked by RBS. TEM results confirmed amorphization (retained amorphized layer of about 187 nm from the surface) of SiC after implantation at RT, which was corroborated by diffused SAD patterns which were obtained from the implanted region. The irradiation of the amorphized layer with 710 MeV Bi^{+51} showed Fresnel contrast, indicating formation of randomly oriented nanocrystallites. Additionally, subjecting the amorphous layer to 710 MeV Bi^{+51} led to epitaxial growth of the amorphous SiC from amorphous-crystalline interface, reducing its thickness from 187 nm to 178 nm. This observed recrystallization was attributed to the substantial maximum electronic energy loss of about 33.7 keV/nm provided by 710 MeV Bi^{+51}. In contrast, SiC implanted at 350 °C retained its structure, but with less and highly defective layers (highly strained layer) of about 70 nm from the surface and 95 nm (from 70 nm below the surface), respectively. Collectively, these layers constituted to a total defective SiC layer of about 165 nm. Meanwhile, subjecting the defective layers to 710 MeV Bi^{+51} led to thickness reduction of 33% in the less defective layer and a decrease of 21% in the highly defective layer. Interestingly, it was noted that the 710 MeV Bi^{+51} irradiation of 350 °C pre-implanted SiC resulted in more extensive recrystallization compared to SiC pre-implanted at RT. The Raman and SEM results confirmed the observed recrystallization of some defects after exposing the damaged layers to electronic energy loss (~33.7 keV/nm). Moreover, the RBS depth profiles indicated that there was no migration of the implanted Se ions was detected after exposing both RT and 350 °C pre-implanted SiC to 710 MeV Bi^{+51} irradiation with maximum electronic energy loss of about 33.7 keV/nm.

CRediT authorship contribution statement

T.S. Mabelane: Writing – review & editing, Visualization, Supervision, Resources, Project administration, Investigation, Conceptualization. **M. Sall:** Validation, Resources, Investigation. **Z.A.Y. Abdalla:** Writing – review & editing, Supervision, Methodology, Investigation. **V. A. Skuratov:** Validation, Resources, Methodology. **T.T. Hlatshwayo:** Writing – original draft, Methodology, Investigation, Formal analysis.

Declaration of competing interest

The authors declare that they have no known competing financial interests or personal relationships that could have appeared to influence the work reported in this paper.

Data availability

Data will be made available on request.

Acknowledgements

Financial support by the National Research Foundation (NRF) of South Africa (Grant numbers: 122894, 120471 and 2204072593) is gratefully acknowledged.

Appendix A. Supplementary data

Supplementary data to this article can be found online at https://doi.org/10.1016/j.vacuum.2024.113189.

References

[1] B.W. Ang, B. Su, Carbon emission intensity in electricity production: a global analysis, Energy Pol. 94 (2016) 56.
[2] A. Midilli, I. Dincer, M. Ay, Green energy strategies for sustainable development, Energy pol 34 (2006) 3623.
[3] Argonne National Laboratory. Radiological and Chemical Fact Sheets to Support Health Risk Analyses for Contaminated areas, Human Health Fact Sheet, August 2005.
[4] A.M. Omer, A review of non-conventional energy systems and environmental pollution control, J. Soil Sci. Environ. Manag. 1 (7) (2010) 127.
[5] J.B. Malherbe, E. Friedland, N.G. Van Der Berg, Ion beam analysis of materials in the PBMR reactor, Nucl. Instrum. Methods Phys. Res., Sect. B 266 (8) (2008) 1373.
[6] report 70, Pebble Bed Modular Reactor, International Atomic Energy Agency, Vienna, Austria, August 2011.
[7] H.A.A. Abdelbagi, V.A. Skuratov, S.A. Adeojo, T.M. Mohlala, T.T. Hlatshwayo, J. B. Malherbe, Effect of SHI irradiation and high temperature annealing on the microstructure of SiC implanted with Ag, Nucl. Instrum. Methods Phys. Res., Sect. B 511 (2022) 18.
[8] Y. Goldberg, M. Levinshtein, S. Rumyantsev, Silicon Carbide (SiC), Properties of Advance Semiconductor Materials, Wiley, 2001.
[9] N.G. van der Berg, J.B. Malherbe, A.J. Botha, E. Friedland, Thermal etching of SiC, Appl. Surf. Sci. 258 (2012) 5561.
[10] T.L. Daulton, T.J. Bernatowicz, R.S. Lewis, S. Messenger, F.J. Stadermann, S. Amari, Polytype distribution of circumstellar silicon carbide: microstructural characterization by transmission electron microscopy, Geochem. Cosmochim. Acta 67 (2003) 4743–4767.
[11] T. Yano, T. Iseki, High-resolution electron microscopy of neutron-irradiation-induced dislocations in SiC, Philos. Mag. A 62 (1990) 421.
[12] H.A.A. Abdelbagia, V.A. Skuratov, S.V. Motloung, E.G. Njoroge, M. Mlambo, J. B. Malherbe, J.H. O'Connell, T.T. Hlatshwayo, Effect of swift heavy ions irradiation in the migration of silver implanted into polycrystalline SiC, Nucl. Instrum. Methods Phys. Res. B. 461 (2019) 201.
[13] T.T. Hlatshwayo, J.H. O'Connell, V.A. Skuratov, M.M. simanga, R.J. Kuhudzai, E. G. Njoroge, J.B. Malherbe, Effect of Xe ion (167 MeV) irradiation on polycrystalline SiC implanted with Kr and Xe at room temperature, J. Phys. D Appl. Phys. 48 (2015) 465306.

[14] A. Audren, A. Benyagoub, L. Thome, F. Garrido, Ion implantation of iodine into silicon carbide: influence of temperature on the produced damage and on the diffusion behaviour, Nucl. Instr. Meth. Phys. Res B. 266 (2008) 2810.
[15] A. Benyagoub, A. Audren, L. Thomé, F. Garrido, Athermal crystallization induced by electronic excitations in ion-irradiated silicon carbide, Appl. Phys. Lett. 89 (2006) 241914.
[16] A. Benyagoub, A. Audren, Mechanism of the swift heavy ion induced epitaxial recrystallization in pre-damaged silicon carbide, J. Appl. Phys. 106 (2009) 08351.
[17] W. Jiang, W.J. Weber, Y. Zhang, S. Thevuthasan, V. Shutthanandan, Ion beam analysis of irradiation effects in 6H–SiC, Nucl. Instrum. Methods Phys. Res. B 207 (2003) 92.
[18] T.T. Hlatshwayo, J.H. O'Connell, V.A. Skuratov, E. Wendler, E.G. Njoroge, M. Mlambo, J.B. Malherbe, Comparative study of the effect of swift heavy ion irradiation at 500 °C and annealing at 500 °C on implanted silicon carbide, RSC Adv. 6 (2016) 68593.
[19] M. Toulemonde, W. Assmann, Y. Zhang, M. Backman, W.J. Weber, C. Dufour, Z. G. Wang, Material transformation: interaction between nuclear and electronic energy losses, Proc. Mat. Scie. 7 (2014) 272.
[20] P. Bienvenu, P. Cassette, G. Andreoletti, M.M. Bé, J. Comte, M.C. Lépy, A new determination of 79Se half-life, App. Rad. Iso. 65 (3) (2007) 355.
[21] B. Ma, M. Kang, Z. Zheng, F. Chen, J. Xie, L. Charlet, C. Liu, The reductive immobilization of aqueous Se(IV) by natural pyrrhotite, J. Harz. Mat. 276 (2014) 422.
[22] Z.A.Y. Abdalla, M.Y.A. Ismail, E.G. Njoroge, E. Wendler, J.B. Malherbe, T. T. Hlatshwayo, Effect of heat treatment on the migration behaviour of selenium implanted into polycrystalline SiC, Nuclear Inst. and, Methods Phys Res B. 487 (2021) 30.
[23] Z.A.Y. Abdalla, E.G. Njoroge, M. Mlambo, S.V. Motloung, J.B. Malherbe, T. T. Hlatshwayo, Isothermal annealing of selenium (Se)-implanted silicon carbide: structural evolution and migration behavior of implanted Se, Mat. Chem. Phys. 276 (2022) 12533.
[24] Z.A.Y. Abdalla, M.Y.A. Ismail, E.G. Njoroge, T.T. Hlatshwayo, E. Wendler, J. B. Malherbe, Migration behaviour of selenium implanted into polycrystalline 3C–SiC, Vacuum 175 (2020) 109235.
[25] E. Friedland, J.B. Malherbe, N.G. van der Berg, T. Hlatshwayo, A.J. Botha, E. Wendler, W. Wesch, Study of silver diffusion in silicon carbide, J. Nucl. Mater. 389 (2009) 326.
[26] J.F. Ziegler, M.D. Ziegler, J.P. Biersack, SRIM–The stopping and range of ions in matter (2010), Nucl. Instrum. Methods Phys. Res. Sect. B Beam Interact. Mater. Atoms 268 (11–12) (2010) 1818.
[27] R. Devanathan, W.J. Weber, Displacement energy surface in 3C and 6H SiC, J. Nucl. Mater. 278 (2000) 258.
[28] F. Gao, W.J. Weber, Cascade overlap and amorphization in (formula presented) Defect accumulation, topological features, and disordering, Phys. Rev. B Condens. Matter. 66 (2002) 1.
[29] J.B. Malherbe, Diffusion of fission products and radiation damage in SiC, J. Phys. D Appl. Phys. 4647 (2013) 473001.
[30] S. Leclerc, M.F. Beaufort, A. Declémy, J.F. Barbot, Strain-induced drift of interstitial atoms in SiC implanted with helium ions at elevated temperature, J. Nucl. Mater. 397 (2010) 132.
[31] S. Lin, Z. Chen, L. Li, C. Yang, Effect of impurities on the Raman scattering of 6H-SiC crystals, Mater. Res.156 (2012) 833.
[32] Z. Xu, Z. He, Y. Song, X. Fu, M. Rommel, X. Luo, A. Hartmaier, J. Zhang, F. Fang, Topic review: application of Raman spectroscopy characterization in micro/nano-machining, Micromach 9 (2018) 361.
[33] H.A.A. Abdelbagi, V.A. Skuratov, S.V. Motloung, E.G. Njoroge, M. Mlambo, T. T. Hlatshwayo, J.B. Malherbe, Effect of swift heavy ions irradiation on the migration behaviour of strontium implanted into polycrystalline SiC, Nucl. Instrum. Methods Phys. Res. B. 451 (2019) 113.